

Thermal vibration analysis of thick laminated plates by the moving least squares differential quadrature method

Lanhe Wu[†]

Department of Engineering Mechanics, Shijiazhuang Railway Institute, Shijiazhuang 050043, P. R. China

(Received November 10, 2004, Accepted November 7, 2005)

Abstract. The stresses and deflections in a laminated rectangular plate under thermal vibration are determined by using the moving least squares differential quadrature (MLSDQ) method based on the first order shear deformation theory. The weighting coefficients used in MLSDQ approximation are obtained through a fast computation of the MLS shape functions and their partial derivatives. By using this method, the governing differential equations are transformed into sets of linear homogeneous algebraic equations in terms of the displacement components at each discrete point. Boundary conditions are implemented through discrete grid points by constraining displacements, bending moments and rotations of the plate. Solving this set of algebraic equations yields the displacement components. Then substituting these displacements into the constitutive equation, we obtain the stresses. The approximate solutions for stress and deflection of laminated plate with cross layer under thermal load are obtained. Numerical results show that the MLSDQ method provides rapidly convergent and accurate solutions for calculating the stresses and deflections in a multi-layered plate of cross ply laminate subjected to thermal vibration of sinusoidal temperature including shear deformation with a few grid points.

Key words: differential quadrature method; moving least-squares method; thermal vibration; laminated plate; shear deformation.

1. Introduction

Laminated plates made of advanced fiber-reinforced composite materials are extensively used in mechanical, civil, nuclear and aerospace structures due to their excellent advantages. As one of the excellent properties, the strength and stiffness of the plate can be tailored to satisfy the given requirements through proper arrangement of stacking sequence, fiber orientation, thickness and material properties of each layer. However, various coupling effects such as stretching-bending, stretching-shearing, and bending-twisting couplings, etc., diminish the stiffness of the plate, and induces many complexities in analyzing behaviors of such plate. Furthermore, composite structures are usually influenced by thermal and moisture environment significantly. So it is very important to have a good understanding of the dynamic behaviors of these structural components in the design and performance evaluation of mechanical systems.

[†] Professor, E-mail: wulanhe1965@yahoo.com.cn

Analytical and numerical techniques for determining the vibration characteristics of laminated plates have been well developed and widely studied. For examples, Baharlou and Leissa (1997) presented an analysis of vibration and buckling of generally laminated plate having various boundary conditions using Ritz method, based on the classical plate theory. Kabir and Chaudhuri (1994, 1999) developed a boundary continuous generalized Navier's approach, and presented an analytical solution for free vibration of arbitrarily laminated plate with clamped and simply supported boundary conditions, in which the effect of shear deformation was considered. However, few of them have been conducted on the thermal vibration analysis of arbitrarily laminated plates. In this area, Wang and his colleagues have made great deal of works in the study of dynamic response of inter-laminar stresses in laminated composite plates under thermal environment (Wang and Zhang 2005, Wang *et al.* 2005). The plane stresses were calculated by using geometric equations and generalized Hooke's law. The interlaminar stresses were evaluated by integrating the 3-D equations of dynamic equilibrium, and utilizing given boundary conditions and continuity conditions between layers. In their studies, the temperature field was assumed to be linear functions of x , y and z , and an exponent function of time t . Based on higher order shear deformation theory and general Von Karman type equation of motion, Huang and Shen (2004) investigated the nonlinear vibration and dynamic response of shear deformable laminated plates in hygrothermal environments. Various factors such as temperature rise, the degree of moisture concentration, the fiber volume fraction on natural frequencies, nonlinear to linear frequency ratios and dynamic response were carefully studied. In their work, the temperature field was assumed to be uniform distribution over the plate surface and through the plate thickness.

In this paper, the response of a simply supported laminated rectangular plate under thermal vibration is studied by employing a novel numerical solution technique, the moving least squares differential quadrature (MLSDQ) method. As an efficient and accurate global solution technique, the differential quadrature (DQ) method were first introduced by Bellman and his associates (1971, 1972), for solving linear and nonlinear differential equations with a little computational cost. Since then, there have been numerous developments and applications of the method in structural mechanics (Bert and Malik 1996, Liew *et al.* 1996, Malik and Bert 1998). However, further application of the method has been greatly restricted by the disadvantage that it cannot be directly used to solve problems with discontinuities or with complex domains, since the grid points used in DQ method must be distributed in a regular manner in order to express the weighting coefficients explicitly. Although these problems can be solved by the domain-superposition technique for discontinuous geometric boundaries and the domain transformation technique for irregular shaped domains, it may cause a significant loss of efficiency and simplicity, especially for problems involving irregular geometries and higher order partial derivatives. To overcome these drawbacks, Liew *et al.* (2002, 2003) developed a new kind of numerical method, the MLSDQ method to solve the static and buckling problems of shear deformable plate. The moving least squares differential quadrature method is a combination of the general differential quadrature method and the element-free Galerkin method. In MLSDQ method, the weighting coefficients of quadrature approximation are calculated directly from the partial derivatives of shape functions used in the element-free Galerkin method. Since the grid points used in moving least squares differential quadrature method can be arbitrarily located, it can be easily used to solve problems having complex domains. In the present paper, this method is employed to study the thermal vibration problems of laminated composite plates having simply supported boundary conditions. The temperature field is assumed to be sinusoidal of coordinates x and y , and of time t , while linearly in the plate thickness direction.

The suitability, efficiency, simplicity and convergence properties of this method are all demonstrated. Also, some new results are presented to study the influence of the relative thickness on the deflection and stress amplitudes of the plate at different time.

2. The MLS-DQ method

Consider a domain in the space Ω discretized by a set of discrete points $\{x_i\}_{i=1,2,\dots,N}$. In the generalized differential quadrature (DQ) or the differential cubature (DC) method. The value of a partial derivative of a certain function $u(x)$ at a discrete point x_i can be approximate as a weighted linear sum of discrete function values chosen within the overall domain of a problem.

$$\mathcal{h}\{u(x)\}_i = \sum_{j=1}^N c_j(x_i)u(x_j) = \sum_{j=1}^N c_{ij}u_j \quad (1)$$

where \mathcal{h} denotes a linear differential operator which can be any orders of partial derivatives or their combinations, c_{ij} are the weighting coefficients, and u_j are the nodal function values. According to Civan (1994), the weighting coefficients c_{ij} can be determined by solving a set of linear algebraic equations which can be obtained by selecting N monomials from a set of polynomial basis and substituting them into Eq. (1). For regular node patterns, explicit expressions of weighting coefficients can be obtained for the first, second and higher derivatives using the Lagrangian interpolation polynomials.

In this paper, the weighting coefficients are directly computed from the partial derivatives of shape functions used in the moving least squares method. Following Belytschko *et al.* (1994), we have

$$u^h(x) = \sum_{i=1}^m p_i(x)a_i(x) = \mathbf{p}^T(x)\mathbf{a}(x) \quad (2)$$

where $p_i(x)$ is a finite set of basis functions and $a_i(x)$ are the unknown coefficients, m denotes the total number of basis functions. In this work on 2-D problems, the intrinsic polynomial basis with $m = 6$ is quadratic, i.e.,

$$\mathbf{p}^T(x) = [1, x, y, x^2, xy, y^2] \quad (3)$$

The coefficients $a_i(x)$ are functions of the spatial coordinates, and they can be obtained by minimizing a weighted, discrete L_2 normal defined as

$$J(\mathbf{a}) = \sum_{i=1}^n \bar{w}_i(x) [\mathbf{p}^T(x_i)\mathbf{a}(x) - u_i]^2 \quad (4)$$

where n is the number of nodes in the neighborhood of x and u_i is the nodal parameter of $u(x)$ at point x_i . $\bar{w}_i(x) = \bar{w}(x-x_i)$ is a positive weight function which decreases as $(x-x_i)$ increases. It always assumes unity at the sampling point x and vanishes outside the domain of influence of x . The size of the domain of influence, or support size, determines the number of discrete points n in the domain of influence.

The extremum of $J(\mathbf{a})$ with respect to $\mathbf{a}(x)$ results in the following linear equations

$$A(x)\mathbf{a}(x) = B(x)u \quad (5)$$

from which

$$\mathbf{a}(x) = A^{-1}(x)B(x)u \quad (6)$$

where

$$A(x) = \sum_{i=1}^n \bar{\omega}_i(x)\mathbf{p}(x_i)\mathbf{p}^T(x_i), \quad B(x) = [B_1(x) \ B_2(x) \ \dots \ B_n(x)]$$

$$B_i(x) = \bar{\omega}_i(x)\mathbf{p}(x_i), \quad u = [u_1 \ u_2 \ \dots \ u_n]^T$$

Substituting Eq. (6) into Eq. (2), the approximate function $u^h(x)$ can then be expressed in terms of the shape function as

$$u^h(x) = \sum_{i=1}^n \phi_i(x)u_i \quad (7)$$

where the nodal shape function $\phi_i(x)$ is given by

$$\phi_i(x) = \mathbf{p}^T(x)A^{-1}(x)B_i(x) \quad (8)$$

Using Eq. (7), the weighting coefficients defined in the DQ method can be computed directly. For instance, we have

$$\frac{\partial u(x)}{\partial x} \approx \frac{\partial u^h(x)}{\partial x} = \sum_{j=1}^n \frac{\partial \phi_j(x)}{\partial x} u_j = \sum_{j=1}^n c_j^{(x)}(x)u_j \quad (9)$$

where $c_j^{(x)}(x)$ is the weighting coefficients of the first order derivative of $u(x)$ in the x direction at any point x with respect to node x_j . If the node x_i is chosen as the sample point, the derivative at this node becomes

$$\left. \frac{\partial u(x)}{\partial x} \right|_{x=x_i} \approx \sum_{j=1}^n \left. \frac{\partial \phi_j(x)}{\partial x} \right|_{x=x_i} u_j = \sum_{j=1}^n c_j^{(x)}(x_i)u_j \quad (10)$$

and the weighting coefficients c_{ij} associated with the first order derivative of $u(x)$ defined in Eq. (1) can be expressed as

$$c_{ij}^{(x)} = c_j^{(x)}(x_i) = \left. \frac{\partial \phi_j(x)}{\partial x} \right|_{x=x_i} \quad (11)$$

Therefore, for each node x_i in the domain, we have the corresponding weighting coefficient of the first derivative, such as $c_{ij}^{(x)}$, which are non-zero only for the points x_j within the support domain of x_i . The weighting coefficients for the other derivatives can be obtained in similar fashion.

3. Determination of weighting coefficients

From Eq. (11), one can obtain the weighting coefficients directly by calculating the partial derivative of shape function $\phi_i(x)$. However, inversions of matrix $A(x)$ and its partial derivatives are too time consuming, and the matrix $A(x)$ will be highly ill-conditioned when a higher basis is used. In order to cut down the computational cost and alleviate the ill-conditioning of matrix $A(x)$, the following numerical procedure is used. First, we define

$$A(x)\lambda(x) = \mathbf{p}(x) \tag{12}$$

then Eq. (8) can be rewritten as

$$\phi_i(x) = \lambda^T(x)B_i(x) \tag{13}$$

Thus, the effort to compute the shape function and its partial derivatives is reduced to the determination of the coefficients vector $\lambda(x)$ and its partial derivatives. The coefficients $\lambda(x)$ can be solved by a normal LU decomposition and back substitution, which requires fewer computations than the inversion of $A(x)$. Moreover, the partial derivatives of $\lambda(x)$ in any order can be calculated by using the same matrix after LU decomposition. For examples, we have

$$A(x)\lambda_{,i}(x) = \mathbf{p}_{,i}(x) - A_{,i}(x)\lambda(x) \tag{14}$$

$$A(x)\lambda_{,ij}(x) = \mathbf{p}_{,ij}(x) - A_{,ij}(x)\lambda(x) - A_{,i,j}(x)\lambda_{,j}(x) - A_{,j,i}(x)\lambda_{,i}(x) \tag{15}$$

So, only back substitution is required to obtain the derivatives of $\lambda(x)$. The weighting coefficients in DQ method can be obtained accordingly using Eqs. (11) and (13).

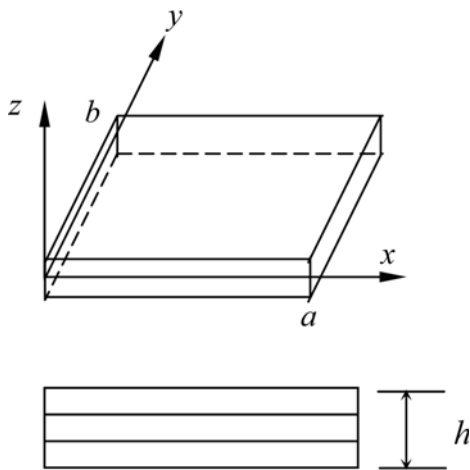


Fig. 1 Geometric and laminate configurations of a rectangular plate

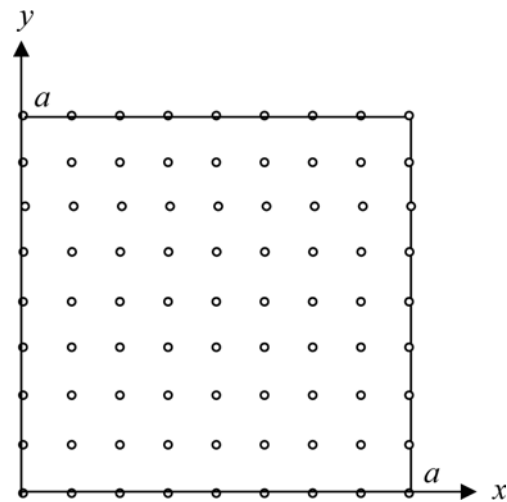


Fig. 2 Regular grid point pattern for square plate problem

4. Basic governing equations

Consider a thick laminated rectangular plate of uniform thickness h , length a and width b as shown in Fig. 1. The displacement fields of the first order shear deformation theory is assumed of the form (Jonnalagadda *et al.* 1994)

$$\begin{aligned}\tilde{u}(x, y, z, t) &= u(x, y, t) + z\psi_1(x, y, t) \\ \tilde{v}(x, y, z, t) &= v(x, y, t) + z\psi_2(x, y, t) \\ \tilde{w}(x, y, z, t) &= w(x, y, t)\end{aligned}\quad (16)$$

where \tilde{u} , \tilde{v} and \tilde{w} are the displacement components along the x , y , z directions, respectively, at point (x, y, z) of the plate thickness; u , v , w denote the displacement components along the x , y , z directions, respectively, at point in the middle plane; ψ_1 , ψ_2 are rotations of the normal about the y , x axes; respectively.

Substituting displacement field (16) into linear strain-displacement relations, yield the strain-displacement relationship

$$\varepsilon_1 = \varepsilon_1^0 + zk_1, \quad \varepsilon_2 = \varepsilon_2^0 + zk_2, \quad \varepsilon_4 = \varepsilon_4^0, \quad \varepsilon_5 = \varepsilon_5^0, \quad \varepsilon_6 = \varepsilon_6^0 + zk_6 \quad (17)$$

where

$$\begin{aligned}\varepsilon_1^0 &= \frac{\partial u}{\partial x}, \quad \varepsilon_2^0 = \frac{\partial v}{\partial y}, \quad \varepsilon_4^0 = \frac{\partial w}{\partial y} + \psi_2, \quad \varepsilon_5^0 = \frac{\partial w}{\partial x} + \psi_1 \\ \varepsilon_6^0 &= \frac{\partial v}{\partial x} + \frac{\partial u}{\partial y}, \quad k_1 = \frac{\partial \psi_1}{\partial x}, \quad k_2 = \frac{\partial \psi_2}{\partial y}, \quad k_6 = \frac{\partial \psi_2}{\partial x} + \frac{\partial \psi_1}{\partial y}\end{aligned}\quad (18)$$

The stress resultants is related to the strain components by

$$\begin{aligned}N_i &= A_{ij}\varepsilon_j^0 + B_{ij}k_j - N_i^T, \quad M_i = B_{ij}\varepsilon_j^0 + D_{ij}k_j - M_i^T \quad (i, j = 1, 2, 6) \\ Q_1 &= A_{44}\varepsilon_4^0 + A_{45}\varepsilon_5^0, \quad Q_2 = A_{45}\varepsilon_4^0 + A_{55}\varepsilon_5^0\end{aligned}\quad (19)$$

where, A_{ij} , B_{ij} , D_{ij} ($i, j = 1, 2, 6$) denote the coefficients of stretching, stretching-bending coupling and bending stiffness, respectively; A_{ij} ($i, j = 4, 5$) denote the coefficients of shearing stiffness. These coefficients are given as

$$(A_{ij}, B_{ij}, D_{ij}) = \sum_{k=1}^n \int_{z_{k-1}}^{z_k} (\bar{Q}_{ij})_{(k)}(1, z, z^2) dz \quad (i, j = 1, 2, 6) \quad (20)$$

$$A_{ij} = \sum_{k=1}^n \int_{z_{k-1}}^{z_k} \mu_p \mu_q (\bar{Q}_{ij})_{(k)} dz \quad (i, j = 4, 5; p = 6 - i, q = 6 - j)$$

where, μ_p and μ_q are shear correction factors. Thermal force resultants N_i^T and M_i^T which corresponding to the temperature change are written as

$$\begin{aligned} \begin{Bmatrix} N_1^T \\ N_2^T \\ N_6^T \end{Bmatrix} &= \sum_{k=1}^n \int_{z_{k-1}}^{z_k} \begin{bmatrix} \bar{Q}_{11} & \bar{Q}_{12} & \bar{Q}_{16} \\ \bar{Q}_{12} & \bar{Q}_{22} & \bar{Q}_{26} \\ \bar{Q}_{16} & \bar{Q}_{26} & \bar{Q}_{26} \end{bmatrix}_{(k)} \begin{Bmatrix} \alpha_x \\ \alpha_y \\ \alpha_{xy} \end{Bmatrix}_{(k)} T dz \\ \begin{Bmatrix} M_1^T \\ M_2^T \\ M_6^T \end{Bmatrix} &= \sum_{k=1}^n \int_{h_{k-1}}^{h_k} \begin{bmatrix} \bar{Q}_{11} & \bar{Q}_{12} & \bar{Q}_{16} \\ \bar{Q}_{12} & \bar{Q}_{22} & \bar{Q}_{26} \\ \bar{Q}_{16} & \bar{Q}_{26} & \bar{Q}_{26} \end{bmatrix}_{(k)} \begin{Bmatrix} \alpha_x \\ \alpha_y \\ \alpha_{xy} \end{Bmatrix}_{(k)} T \cdot z dz \end{aligned} \quad (21)$$

where α_x and α_y are the coefficients of thermal expansion, α_{xy} is the coefficient of thermal shear. Based on the first order shear deformation theory, the dynamic equilibrium equation of the plate under thermal load given in terms of the plate displacements is expressed as Whitney (1987).

$$\begin{bmatrix} L_{11} & L_{12} & L_{13} & L_{14} & L_{15} \\ L_{12} & L_{22} & L_{23} & L_{24} & L_{25} \\ L_{13} & L_{23} & L_{33} & L_{34} & L_{35} \\ L_{14} & L_{24} & L_{34} & L_{44} & L_{45} \\ L_{15} & L_{25} & L_{35} & L_{45} & L_{55} \end{bmatrix} \begin{Bmatrix} u \\ v \\ w \\ \psi_1 \\ \psi_2 \end{Bmatrix} = \begin{Bmatrix} P_1 \\ P_2 \\ P_3 \\ P_4 \\ P_5 \end{Bmatrix} \quad (22)$$

where L_{ij} , respectively, are the linear differential operators such as

$$\begin{aligned} L_{11} &= A_{11} \frac{\partial^2}{\partial x^2} + 2A_{16} \frac{\partial^2}{\partial x \partial y} + A_{66} \frac{\partial^2}{\partial y^2} - I_1 \frac{\partial^2}{\partial t^2}, & L_{12} &= A_{16} \frac{\partial^2}{\partial x^2} + (A_{12} + A_{66}) \frac{\partial^2}{\partial x \partial y} + A_{26} \frac{\partial^2}{\partial y^2} \\ L_{14} &= B_{11} \frac{\partial^2}{\partial x^2} + 2B_{16} \frac{\partial^2}{\partial x \partial y} + B_{66} \frac{\partial^2}{\partial y^2} - I_2 \frac{\partial^2}{\partial t^2}, & L_{15} &= B_{16} \frac{\partial^2}{\partial x^2} + (B_{12} + B_{66}) \frac{\partial^2}{\partial x \partial y} + B_{26} \frac{\partial^2}{\partial y^2} \\ L_{22} &= A_{66} \frac{\partial^2}{\partial x^2} + 2A_{26} \frac{\partial^2}{\partial x \partial y} + A_{22} \frac{\partial^2}{\partial y^2} - I_1 \frac{\partial^2}{\partial t^2}, & L_{24} &= B_{16} \frac{\partial^2}{\partial x^2} + (B_{12} + B_{66}) \frac{\partial^2}{\partial x \partial y} + B_{26} \frac{\partial^2}{\partial y^2} \\ L_{25} &= B_{66} \frac{\partial^2}{\partial x^2} + 2B_{26} \frac{\partial^2}{\partial x \partial y} + B_{22} \frac{\partial^2}{\partial y^2} - I_2 \frac{\partial^2}{\partial t^2}, & L_{33} &= -A_{55} \frac{\partial^2}{\partial x^2} - 2A_{45} \frac{\partial^2}{\partial x \partial y} - A_{44} \frac{\partial^2}{\partial y^2} + I_1 \frac{\partial^2}{\partial t^2} \\ L_{34} &= -A_{55} \frac{\partial}{\partial x} - A_{45} \frac{\partial}{\partial y}, & L_{35} &= -A_{45} \frac{\partial}{\partial x} - A_{44} \frac{\partial}{\partial y}, & L_{44} &= D_{11} \frac{\partial^2}{\partial x^2} + 2D_{16} \frac{\partial^2}{\partial x \partial y} + D_{66} \frac{\partial^2}{\partial y^2} - I_3 \frac{\partial^2}{\partial t^2} \\ L_{45} &= D_{16} \frac{\partial^2}{\partial x^2} + (D_{12} + D_{66}) \frac{\partial^2}{\partial x \partial y} + D_{26} \frac{\partial^2}{\partial y^2}, & L_{55} &= D_{66} \frac{\partial^2}{\partial x^2} + 2D_{26} \frac{\partial^2}{\partial x \partial y} + D_{22} \frac{\partial^2}{\partial y^2} - I_3 \frac{\partial^2}{\partial t^2} \\ L_{13} &= L_{23} = 0 \end{aligned} \quad (23)$$

where $I_i (i = 1, 2, 3)$ are moments of inertia defined as

$$(I_1, I_2, I_3) = \int_{-h/2}^{h/2} \rho(1, z, z^2) dz \quad (24)$$

where, ρ denotes density of a layer. P_i ($i = 1, 2, \dots, 5$) are the combinations of the partial derivatives of the temperature force resultants with respect to x and y , which are as follows

$$P_1 = \frac{\partial N_1^T}{\partial x} + \frac{\partial N_6^T}{\partial y}, \quad P_2 = \frac{\partial N_6^T}{\partial x} + \frac{\partial N_2^T}{\partial y}, \quad P_3 = 0, \quad P_4 = \frac{\partial M_1^T}{\partial x} + \frac{\partial M_6^T}{\partial y}, \quad P_5 = \frac{\partial M_6^T}{\partial x} + \frac{\partial M_2^T}{\partial y} \quad (25)$$

For no heat generation, linear and uncouple case of thermo-mechanics, the temperature distribution in the plate is governed by the following steady state heat conduction equation (Hetnaski 1986)

$$K \left(\frac{\partial^2 T}{\partial x^2} + \frac{\partial^2 T}{\partial y^2} + \frac{\partial^2 T}{\partial z^2} \right) = \frac{\partial T}{\partial t} \quad (26)$$

where K is the coefficient of thermal conductivity.

In this work, the time-dependent temperature difference T is assumed linear in the thickness direction and is designated by $T = T_0(x, y, t) + (z/h)T_1(x, y, t)$. For simplicity of computation, we further assume T is a sinusoidal function in the plate plane, i.e.,

$$T = (z/h)\tilde{T}\sin(\pi x/a)\sin(\pi y/b)\sin\zeta t \quad (27)$$

where ζ is the frequency of applied heat flux. Substituting Eq. (27) into Eq. (26), one obtains

$$\tan\zeta t = -\frac{a^2\zeta}{K\pi^2(1+a^2/b^2)} \quad (28)$$

From this equation, we can find the frequency of applied heat flux ζ for the given values a/b and K at any time.

The simply supported boundary conditions for a thick rectangular plate are expressed as (takes the edges $x = 0, a$ as an example)

$$u = 0, v = 0, w = 0, \psi_2 = 0, M_1 = 0 \quad (29)$$

When the plate vibrates harmonically, all the physical resultants can be written as harmonic functions of t . Thus the displacement components are written as

$$u = U\sin\omega_{mn}t, \quad v = V\sin\omega_{mn}t, \quad w = W\sin\omega_{mn}t, \quad \psi_1 = \Theta_1\sin\omega_{mn}t, \quad \psi_2 = \Theta_2\sin\omega_{mn}t \quad (30)$$

where ω_{mn} is the angular frequency. Substituting these equations into Eq. (3), one obtains

$$\begin{bmatrix} L_{11} + \omega_{mn}^2 I_1 & L_{12} & L_{13} & L_{14} + \omega_{mn}^2 I_2 & L_{15} \\ L_{12} & L_{22} + \omega_{mn}^2 I_1 & L_{23} & L_{24} & L_{25} + \omega_{mn}^2 I_2 \\ L_{13} & L_{23} & L_{33} - \omega_{mn}^2 I_1 & L_{34} & L_{35} \\ L_{14} + \omega_{mn}^2 I_2 & L_{24} & L_{34} & L_{44} + \omega_{mn}^2 I_3 & L_{45} \\ L_{15} & L_{25} + \omega_{mn}^2 I_2 & L_{35} & L_{45} & L_{55} + \omega_{mn}^2 I_3 \end{bmatrix} \begin{Bmatrix} U \\ V \\ W \\ \Theta_1 \\ \Theta_2 \end{Bmatrix} \sin\omega_{mn}t = \begin{Bmatrix} F_1 \\ F_2 \\ F_3 \\ F_4 \\ F_5 \end{Bmatrix} \sin\zeta t \quad (31)$$

where

$$\begin{aligned}
F_1 &= \sum_{k=1}^n [\bar{Q}_{11}^{(k)} \alpha_x^{(k)} + \bar{Q}_{12}^{(k)} \alpha_y^{(k)} + \bar{Q}_{16}^{(k)} \alpha_{xy}^{(k)}] \frac{\pi \tilde{T}}{2ah} (z_k^2 - z_{k-1}^2) \cos \frac{\pi x}{a} \sin \frac{\pi y}{b} \\
&\quad + \sum_{k=1}^n [\bar{Q}_{16}^{(k)} \alpha_x^{(k)} + \bar{Q}_{26}^{(k)} \alpha_y^{(k)} + \bar{Q}_{66}^{(k)} \alpha_{xy}^{(k)}] \frac{\pi \tilde{T}}{2bh} (z_k^2 - z_{k-1}^2) \sin \frac{\pi x}{a} \cos \frac{\pi y}{b} \\
F_2 &= \sum_{k=1}^n [\bar{Q}_{16}^{(k)} \alpha_x^{(k)} + \bar{Q}_{26}^{(k)} \alpha_y^{(k)} + \bar{Q}_{66}^{(k)} \alpha_{xy}^{(k)}] \frac{\pi \tilde{T}_1}{2ah} (z_k^2 - z_{k-1}^2) \cos \frac{\pi x}{a} \sin \frac{\pi y}{b} \\
&\quad + \sum_{k=1}^n [\bar{Q}_{12}^{(k)} \alpha_x^{(k)} + \bar{Q}_{22}^{(k)} \alpha_y^{(k)} + \bar{Q}_{26}^{(k)} \alpha_{xy}^{(k)}] \frac{\pi \tilde{T}}{2bh} (z_k^2 - z_{k-1}^2) \sin \frac{\pi x}{a} \cos \frac{\pi y}{b} \\
F_3 &= 0 \\
F_4 &= \sum_{k=1}^n [\bar{Q}_{11}^{(k)} \alpha_x^{(k)} + \bar{Q}_{12}^{(k)} \alpha_y^{(k)} + \bar{Q}_{16}^{(k)} \alpha_{xy}^{(k)}] \frac{\pi \tilde{T}}{3ah} (z_k^3 - z_{k-1}^3) \cos \frac{\pi x}{a} \sin \frac{\pi y}{b} \\
&\quad + \sum_{k=1}^n [\bar{Q}_{16}^{(k)} \alpha_x^{(k)} + \bar{Q}_{26}^{(k)} \alpha_y^{(k)} + \bar{Q}_{66}^{(k)} \alpha_{xy}^{(k)}] \frac{\pi \tilde{T}}{3bh} (z_k^3 - z_{k-1}^3) \sin \frac{\pi x}{a} \cos \frac{\pi y}{b} \\
F_5 &= \sum_{k=1}^n [\bar{Q}_{16}^{(k)} \alpha_x^{(k)} + \bar{Q}_{26}^{(k)} \alpha_y^{(k)} + \bar{Q}_{66}^{(k)} \alpha_{xy}^{(k)}] \frac{\pi \tilde{T}}{3ah} (z_k^3 - z_{k-1}^3) \cos \frac{\pi x}{a} \sin \frac{\pi y}{b} \\
&\quad + \sum_{k=1}^n [\bar{Q}_{12}^{(k)} \alpha_x^{(k)} + \bar{Q}_{22}^{(k)} \alpha_y^{(k)} + \bar{Q}_{26}^{(k)} \alpha_{xy}^{(k)}] \frac{\pi \tilde{T}}{3bh} (z_k^3 - z_{k-1}^3) \sin \frac{\pi x}{a} \cos \frac{\pi y}{b} \tag{32}
\end{aligned}$$

Substituting Eq. (30) into Eq. (29), the boundary condition can be written as (takes the edges $x=0$, a as an example)

$$\begin{aligned}
U &= 0, \quad V = 0, \quad W = 0, \quad \Theta_2 = 0, \\
B_{11} \frac{\partial U}{\partial x} + B_{16} \frac{\partial U}{\partial y} + B_{16} \frac{\partial V}{\partial x} + B_{12} \frac{\partial V}{\partial y} + D_{11} \frac{\partial \Theta_1}{\partial x} + D_{16} \frac{\partial \Theta_1}{\partial y} + D_{16} \frac{\partial \Theta_2}{\partial x} + D_{12} \frac{\partial \Theta_2}{\partial y} &= 0 \tag{33}
\end{aligned}$$

The stresses in the k th layer are expressed as

$$\begin{aligned}
\sigma_x^{(k)} &= \left\{ \bar{Q}_{11}^{(k)} \left(\frac{\partial U}{\partial x} + \frac{\partial \Theta_1}{\partial x} z - \alpha_x^{(k)} T \right) + \bar{Q}_{12}^{(k)} \left(\frac{\partial V}{\partial y} + \frac{\partial \Theta_1}{\partial y} z - \alpha_y^{(k)} T \right) \right. \\
&\quad \left. + \bar{Q}_{16}^{(k)} \left[\frac{\partial U}{\partial y} + \frac{\partial V}{\partial x} + \left(\frac{\partial \Theta_1}{\partial y} + \frac{\partial \Theta_2}{\partial x} \right) z - \alpha_{xy}^{(k)} T \right] \right\} \sin \omega_{mn} t
\end{aligned}$$

$$\begin{aligned}
\sigma_y^{(k)} &= \left\{ \bar{Q}_{12}^{(k)} \left(\frac{\partial U}{\partial x} + \frac{\partial \Theta_1}{\partial x} z - \alpha_x^{(k)} T \right) + \bar{Q}_{22}^{(k)} \left(\frac{\partial V}{\partial y} + \frac{\partial \Theta_1}{\partial y} z - \alpha_y^{(k)} T \right) \right. \\
&\quad \left. + \bar{Q}_{26}^{(k)} \left[\frac{\partial U}{\partial y} + \frac{\partial V}{\partial x} + \left(\frac{\partial \Theta_1}{\partial y} + \frac{\partial \Theta_2}{\partial x} \right) z - \alpha_{xy}^{(k)} T \right] \right\} \sin \omega_{mn} t \\
\sigma_{xy}^{(k)} &= \left\{ \bar{Q}_{16}^{(k)} \left(\frac{\partial U}{\partial x} + \frac{\partial \Theta_1}{\partial x} z - \alpha_x^{(k)} T \right) + \bar{Q}_{26}^{(k)} \left(\frac{\partial V}{\partial y} + \frac{\partial \Theta_1}{\partial y} z - \alpha_y^{(k)} T \right) \right. \\
&\quad \left. + \bar{Q}_{66}^{(k)} \left[\frac{\partial U}{\partial y} + \frac{\partial V}{\partial x} + \left(\frac{\partial \Theta_1}{\partial y} + \frac{\partial \Theta_2}{\partial x} \right) z - \alpha_{xy}^{(k)} T \right] \right\} \sin \omega_{mn} t \\
\sigma_{yz}^{(k)} &= \left\{ \bar{Q}_{44}^{(k)} \left(\frac{\partial W}{\partial y} + \Theta_2 \right) + \bar{Q}_{45}^{(k)} \left(\frac{\partial W}{\partial x} + \Theta_1 \right) \right\} \sin \omega_{mn} t \\
\sigma_{xz}^{(k)} &= \left\{ \bar{Q}_{45}^{(k)} \left(\frac{\partial W}{\partial y} + \Theta_2 \right) + \bar{Q}_{55}^{(k)} \left(\frac{\partial W}{\partial x} + \Theta_1 \right) \right\} \sin \omega_{mn} t
\end{aligned} \tag{34}$$

5. Discretization of governing equations and boundary conditions

Now, let's discrete the governing equations and the boundary condition equations. First, the plate is discreted by a finite number of nodes (x_i, y_i) , each of which are associated with five nodal parameters $(U^i, V^i, W^i, \Theta_1^i, \Theta_2^i)$. Then, a circle of influence can be formed for each discrete point and the moving least-squares approximation of the displacement components are achieved in the domain of influence as described in section 2:

$$\begin{aligned}
U^h(x, y) &= \sum_{i=1}^n \phi_i(x, y) U^i, \quad V^h(x, y) = \sum_{i=1}^n \phi_i(x, y) V^i, \quad W^h(x, y) = \sum_{i=1}^n \phi_i(x, y) W^i \\
\Theta_1^h(x, y) &= \sum_{i=1}^n \phi_i(x, y) \Theta_1^i, \quad \Theta_2^h(x, y) = \sum_{i=1}^n \phi_i(x, y) \Theta_2^i
\end{aligned} \tag{35}$$

where n is the number of nodes within the domain of influence. It should be noted that n is dependent on the support size and may be different when different nodes are considered. One should also note that the nodal parameters are not equal to the physical values at the corresponding node. This is due to the shape functions used in the moving least squares method do not satisfy the Kronecker's delta condition generally, i.e., $\phi_i(x_j, y_j) \neq \delta_{ij}$. Therefore, we have

$$\begin{aligned}
U(x_i, y_i) &\approx U^h(x_i, y_i) = \sum_{j=1}^n \phi_j(x_i, y_i) U^j = \sum_{j=1}^n \phi_{ij} U^j \\
V(x_i, y_i) &\approx V^h(x_i, y_i) = \sum_{j=1}^n \phi_j(x_i, y_i) V^j = \sum_{j=1}^n \phi_{ij} V^j
\end{aligned}$$

$$\begin{aligned}
 W(x_i, y_i) &\approx W^h(x_i, y_i) = \sum_{j=1}^n \phi_j(x_i, y_i) W^j = \sum_{j=1}^n \phi_{ij} W^j \\
 \Theta_1(x_i, y_i) &\approx \Theta_1^h(x_i, y_i) = \sum_{j=1}^n \phi_j(x_i, y_i) \Theta_1^j = \sum_{j=1}^n \phi_{ij} \Theta_1^j \\
 \Theta_2(x_i, y_i) &\approx \Theta_2^h(x_i, y_i) = \sum_{j=1}^n \phi_j(x_i, y_i) \Theta_2^j = \sum_{j=1}^n \phi_{ij} \Theta_2^j
 \end{aligned} \tag{36}$$

where $\phi_{ij} = \phi_j(x_i, y_i)$ for simplicity.

The shape function $\phi_i(x, y)$ and its partial derivatives can be calculated by the fast computation technique as described in section 3. Thereafter, the weighting coefficients with respect to any order of partial derivatives of the approximate displacement components can be obtained directly. The following expressions give the first- and second-order partial derivatives of transverse deflection component in terms of the DQ discretization:

$$\begin{aligned}
 \frac{\partial W}{\partial x} &\approx \frac{\partial W^h(x, y)}{\partial x} = \sum_{i=1}^n \frac{\partial \phi_i(x, y)}{\partial x} W^i = \sum_{i=1}^n c_i^{(x)}(x, y) W^i \\
 \frac{\partial W}{\partial y} &\approx \frac{\partial W^h(x, y)}{\partial y} = \sum_{i=1}^n \frac{\partial \phi_i(x, y)}{\partial y} W^i = \sum_{i=1}^n c_i^{(y)}(x, y) W^i \\
 \frac{\partial^2 W}{\partial x^2} &\approx \frac{\partial^2 W^h(x, y)}{\partial x^2} = \sum_{i=1}^n \frac{\partial^2 \phi_i(x, y)}{\partial x^2} W^i = \sum_{i=1}^n c_i^{(xx)}(x, y) W^i \\
 \frac{\partial^2 W}{\partial y^2} &\approx \frac{\partial^2 W^h(x, y)}{\partial y^2} = \sum_{i=1}^n \frac{\partial^2 \phi_i(x, y)}{\partial y^2} W^i = \sum_{i=1}^n c_i^{(yy)}(x, y) W^i \\
 \frac{\partial^2 W}{\partial x \partial y} &\approx \frac{\partial^2 W^h(x, y)}{\partial x \partial y} = \sum_{i=1}^n \frac{\partial^2 \phi_i(x, y)}{\partial x \partial y} W^i = \sum_{i=1}^n c_i^{(xy)}(x, y) W^i
 \end{aligned} \tag{37}$$

Similarly, we have the DQ discretization for other four displacement components. Substituting these equations into the governing Eq. (31), we obtain the discrete forms of governing equations at point (x_i, y_i) as

$$\sum_{j=1}^n \begin{bmatrix} \mathfrak{R}_{11}^j & \mathfrak{R}_{12}^j & \mathfrak{R}_{13}^j & \mathfrak{R}_{14}^j & \mathfrak{R}_{15}^j \\ \mathfrak{R}_{12}^j & \mathfrak{R}_{22}^j & \mathfrak{R}_{23}^j & \mathfrak{R}_{24}^j & \mathfrak{R}_{25}^j \\ \mathfrak{R}_{13}^j & \mathfrak{R}_{23}^j & \mathfrak{R}_{33}^j & \mathfrak{R}_{34}^j & \mathfrak{R}_{35}^j \\ \mathfrak{R}_{14}^j & \mathfrak{R}_{24}^j & \mathfrak{R}_{34}^j & \mathfrak{R}_{44}^j & \mathfrak{R}_{45}^j \\ \mathfrak{R}_{15}^j & \mathfrak{R}_{25}^j & \mathfrak{R}_{35}^j & \mathfrak{R}_{45}^j & \mathfrak{R}_{55}^j \end{bmatrix} \begin{Bmatrix} U^j \\ V^j \\ W^j \\ \Theta_1^j \\ \Theta_2^j \end{Bmatrix} \sin \omega_{mn} t = \begin{Bmatrix} F_1(x_i, y_i) \\ F_2(x_i, y_i) \\ F_3(x_i, y_i) \\ F_4(x_i, y_i) \\ F_5(x_i, y_i) \end{Bmatrix} \sin \zeta t \tag{38}$$

where the coefficients $\mathfrak{R}_{pq}^j (p, q = 1, 2, \dots, 5)$ are as follows

$$\begin{aligned}
\mathfrak{R}_{11}^j &= A_{11}c_{ij}^{(xx)} + 2A_{16}c_{ij}^{(xy)} + A_{66}c_{ij}^{(yy)} + \omega_{mn}^2 I_1 \phi_{ij} \\
\mathfrak{R}_{12}^j &= A_{16}c_{ij}^{(xx)} + (A_{12} + A_{66})c_{ij}^{(xy)} + A_{26}c_{ij}^{(yy)}, \quad \mathfrak{R}_{13}^j = \mathfrak{R}_{23}^j = 0 \\
\mathfrak{R}_{14}^j &= B_{11}c_{ij}^{(xx)} + 2B_{16}c_{ij}^{(xy)} + B_{66}c_{ij}^{(yy)} + \omega_{mn}^2 I_2 \phi_{ij}, \quad \mathfrak{R}_{15}^j = B_{16}c_{ij}^{(xx)} + (B_{12} + B_{66})c_{ij}^{(xy)} + B_{26}c_{ij}^{(yy)} \\
\mathfrak{R}_{22}^j &= A_{66}c_{ij}^{(xx)} + 2A_{26}c_{ij}^{(xy)} + A_{22}c_{ij}^{(yy)} + \omega_{mn}^2 I_1 \phi_{ij}, \quad \mathfrak{R}_{24}^j = B_{16}c_{ij}^{(xx)} + (B_{12} + B_{66})c_{ij}^{(xy)} + B_{26}c_{ij}^{(yy)} \\
\mathfrak{R}_{25}^j &= B_{66}c_{ij}^{(xx)} + 2B_{26}c_{ij}^{(xy)} + B_{22}c_{ij}^{(yy)} + \omega_{mn}^2 I_2 \phi_{ij}, \quad \mathfrak{R}_{33}^j = -A_{55}c_{ij}^{(xx)} - 2A_{45}c_{ij}^{(xy)} - A_{44}c_{ij}^{(yy)} - \omega_{mn}^2 I_1 \phi_{ij} \\
\mathfrak{R}_{34}^j &= -A_{55}c_{ij}^{(x)} - A_{45}c_{ij}^{(y)}, \quad \mathfrak{R}_{35}^j = -A_{45}c_{ij}^{(x)} - A_{44}c_{ij}^{(y)}, \quad \mathfrak{R}_{44}^j = D_{11}c_{ij}^{(xx)} + 2D_{16}c_{ij}^{(xy)} + D_{66}c_{ij}^{(yy)} + \omega_{mn}^2 I_3 \phi_{ij} \\
\mathfrak{R}_{45}^j &= D_{16}c_{ij}^{(xx)} + (D_{12} + D_{66})c_{ij}^{(xy)} + D_{26}c_{ij}^{(yy)}, \quad \mathfrak{R}_{55}^j = D_{66}c_{ij}^{(xx)} + 2D_{26}c_{ij}^{(xy)} + D_{22}c_{ij}^{(yy)} + \omega_{mn}^2 I_3 \phi_{ij} \quad (39)
\end{aligned}$$

Similarly, the boundary condition Eq. (33) can be discreted as

$$\begin{aligned}
\sum_{j=1}^n \phi_{ij} U^j = 0, \quad \sum_{j=1}^n \phi_{ij} V^j = 0, \quad \sum_{j=1}^n \phi_{ij} W^j = 0, \quad \sum_{j=1}^n \phi_{ij} \Theta_2^j = 0 \\
B_{11} \sum_{j=1}^n c_{ij}^{(x)} U^j + B_{16} \sum_{j=1}^n c_{ij}^{(y)} U^j + B_{16} \sum_{j=1}^n c_{ij}^{(x)} V^j + B_{12} \sum_{j=1}^n c_{ij}^{(y)} V^j \\
+ D_{11} \sum_{j=1}^n c_{ij}^{(x)} \Theta_1^j + D_{16} \sum_{j=1}^n c_{ij}^{(y)} \Theta_1^j + D_{16} \sum_{j=1}^n c_{ij}^{(x)} \Theta_2^j + D_{12} \sum_{j=1}^n c_{ij}^{(y)} \Theta_2^j = 0 \quad (40)
\end{aligned}$$

where i is the index number of the points on boundary.

Also, the stresses in the k th layer at point (x_i, y_i) are discreted as

$$\begin{aligned}
\sigma_{xi}^{(k)} &= \left\{ \bar{Q}_{11}^{(k)} \left(\sum_{j=1}^n c_{ij}^{(x)} U^j + z \sum_{j=1}^n c_{ij}^{(x)} \Theta_1^j - \alpha_x^{(k)} T \right) + \bar{Q}_{12}^{(k)} \left(\sum_{j=1}^n c_{ij}^{(y)} V^j + z \sum_{j=1}^n c_{ij}^{(y)} \Theta_1^j - \alpha_y^{(k)} T \right) \right. \\
&\quad \left. + \bar{Q}_{16}^{(k)} \left[\sum_{j=1}^n c_{ij}^{(y)} U^j + \sum_{j=1}^n c_{ij}^{(x)} V^j + z \left(\sum_{j=1}^n c_{ij}^{(y)} \Theta_1^j + \sum_{j=1}^n c_{ij}^{(x)} \Theta_2^j \right) - \alpha_{xy}^{(k)} T \right] \right\} \sin \omega_{mn} t \\
\sigma_{yi}^{(k)} &= \left\{ \bar{Q}_{12}^{(k)} \left(\sum_{j=1}^n c_{ij}^{(x)} U^j + z \sum_{j=1}^n c_{ij}^{(x)} \Theta_1^j - \alpha_x^{(k)} T \right) + \bar{Q}_{22}^{(k)} \left(\sum_{j=1}^n c_{ij}^{(y)} V^j + z \sum_{j=1}^n c_{ij}^{(y)} \Theta_1^j - \alpha_y^{(k)} T \right) \right. \\
&\quad \left. + \bar{Q}_{26}^{(k)} \left[\sum_{j=1}^n c_{ij}^{(y)} U^j + \sum_{j=1}^n c_{ij}^{(x)} V^j + z \left(\sum_{j=1}^n c_{ij}^{(y)} \Theta_1^j + \sum_{j=1}^n c_{ij}^{(x)} \Theta_2^j \right) - \alpha_{xy}^{(k)} T \right] \right\} \sin \omega_{mn} t \\
\sigma_{xyi}^{(k)} &= \left\{ \bar{Q}_{16}^{(k)} \left(\sum_{j=1}^n c_{ij}^{(x)} U^j + z \sum_{j=1}^n c_{ij}^{(x)} \Theta_1^j - \alpha_x^{(k)} T \right) + \bar{Q}_{26}^{(k)} \left(\sum_{j=1}^n c_{ij}^{(y)} V^j + z \sum_{j=1}^n c_{ij}^{(y)} \Theta_1^j - \alpha_y^{(k)} T \right) \right.
\end{aligned}$$

$$\begin{aligned}
& + \bar{Q}_{66}^{(k)} \left[\sum_{j=1}^n c_{ij}^{(y)} U^j + \sum_{j=1}^n c_{ij}^{(x)} V^j + \left(\sum_{j=1}^n c_{ij}^{(y)} \Theta_1^j + \sum_{j=1}^n c_{ij}^{(x)} \Theta_2^j \right) - \alpha_{xy}^{(k)} T \right] \sin \omega_{mn} t \\
\sigma_{yzi}^{(k)} & = \left\{ \bar{Q}_{44}^{(k)} \left(\sum_{j=1}^n c_{ij}^{(y)} W^j + \sum_{j=1}^n \phi_{ij} \Theta_2^j \right) + \bar{Q}_{45}^{(k)} \left(\sum_{j=1}^n c_{ij}^{(x)} W^j + \sum_{j=1}^n \phi_{ij} \Theta_1^j \right) \right\} \sin \omega_{mn} t \\
\sigma_{xzi}^{(k)} & = \left\{ \bar{Q}_{45}^{(k)} \left(\sum_{j=1}^n c_{ij}^{(y)} W^j + \sum_{j=1}^n \phi_{ij} \Theta_2^j \right) + \bar{Q}_{55}^{(k)} \left(\sum_{j=1}^n c_{ij}^{(x)} W^j + \sum_{j=1}^n \phi_{ij} \Theta_1^j \right) \right\} \sin \omega_{mn} t \quad (41)
\end{aligned}$$

6. Natural frequency

The natural frequency of a simply supported laminated plate can be easily determined by assuming the displacement components as sinusoidal functions

$$\begin{aligned}
u & = a_{mn} \cos(m\pi x/a) \sin(n\pi y/b) \sin \omega_{mn} t, \quad v = b_{mn} \sin(m\pi x/a) \cos(n\pi y/b) \sin \omega_{mn} t \\
w & = c_{mn} \sin(m\pi x/a) \sin(n\pi y/b) \sin \omega_{mn} t, \quad \psi_1 = d_{mn} \cos(m\pi x/a) \sin(n\pi y/b) \sin \omega_{mn} t \\
\psi_2 & = e_{mn} \sin(m\pi x/a) \cos(n\pi y/b) \sin \omega_{mn} t \quad (42)
\end{aligned}$$

Substituting these equations into the dynamic Eq. (22) and setting

$$P_1 = 0, \quad P_2 = 0, \quad P_3 = 0, \quad P_4 = 0, \quad P_5 = 0 \quad (43)$$

we have

$$\begin{bmatrix} S_{11} - \lambda_{mn} & S_{12} & 0 & 0 & 0 \\ S_{12} & S_{22} - \lambda_{mn} & 0 & 0 & 0 \\ 0 & 0 & S_{33} - \lambda_{mn} & S_{34} & S_{35} \\ 0 & 0 & S_{34} & S_{44} - h^3 \lambda_{mn}/12 & S_{45} \\ 0 & 0 & S_{35} & S_{45} & S_{55} - h^3 \lambda_{mn}/12 \end{bmatrix} \begin{Bmatrix} a_{mn} \\ b_{mn} \\ c_{mn} \\ d_{mn} \\ e_{mn} \end{Bmatrix} = \begin{Bmatrix} 0 \\ 0 \\ 0 \\ 0 \\ 0 \end{Bmatrix} \quad (44)$$

where $\lambda_{mn} = \rho \omega_{mn}^2$,

$$S_{11} = A_{11}(m\pi/a)^2 + A_{66}(n\pi/b)^2, \quad S_{12} = (A_{12} + A_{66})(m\pi/a)(n\pi/b)$$

$$S_{22} = A_{66}(m\pi/a)^2 + A_{22}(n\pi/b)^2, \quad S_{33} = A_{55}(m\pi/a)^2 + A_{44}(n\pi/b)^2$$

$$S_{34} = A_{55}(m\pi/a), \quad S_{35} = A_{44}(n\pi/b), \quad S_{44} = D_{11}(m\pi/a)^2 + D_{66}(n\pi/b)^2 + A_{55}$$

$$S_{45} = (D_{12} + D_{66})(m\pi/a)(n\pi/b), \quad S_{55} = D_{66}(m\pi/a)^2 + D_{22}(n\pi/b)^2 + A_{44}$$

If the plate is vibrating in a certain frequency, Eq. (44) must have non-trivial solutions. Thus the determinant of coefficient matrix in homogeneous Eq. (44) must be zero, and we can find the frequency ω_{mn} corresponding to each mode shape.

7. Numerical results and discussion

Combining the discretized governing Eq. (38) at each discrete point in the physical domain and the boundary condition (40) at each boundary point, and rewriting them in terms of matrix form, we obtain

$$[K]\{\Delta\} = \{R\} \quad (45)$$

where $[K]$ is the bending stiffness matrix ; $\{\Delta\}$ is the displacement vector, which is expressed as

$$\{\Delta\} = \{U^1, V^1, W^1, \Theta_1^1, \Theta_2^1, U^2, V^2, W^2, \Theta_1^2, \Theta_2^2, \dots, U^N, V^N, W^N, \Theta_1^N, \Theta_2^N\}^T \quad (46)$$

where N is the total number of grid points in the overall domain. Solving the linear algebraic Eq. (45), we can obtain the displacements vector. Moreover, the stresses of the plate can be obtained.

To demonstrate the applicability and efficiency of the MLSDQ method for thermal vibration analysis of laminated plates, numerical calculations have been performed for a laminated plate with three cross plies under simply supported boundary conditions. Material properties are

$$E_1 = 25E_2, \quad G_{12} = G_{13} = 0.5E_2, \quad G_{23} = 0.2E_2, \quad \nu_{12} = \nu_{13} = 0.25 \\ \alpha_x = 10^{-6}, \quad \alpha_y = 3 \times 10^{-6}, \quad K = 0.14$$

The temperature change is $\tilde{T} = 100$. In our present work, the following weighing function is used

$$\bar{w}_i(x, y) = \begin{cases} e^{-(2.5s)^2} & s \leq 1 \\ 0 & s > 1 \end{cases} \quad (47)$$

where $s = \sqrt{(x - x_i)^2 + (y - y_i)^2}/r$ is the dimensionless distance from a discrete node (x_i, y_i) to a sampling point (x, y) in the domain of support with radius r . For convenience of presentation, a scaling factor d_{\max} is defined by

$$d_{\max} = r/h_m \quad (48)$$

where h_m is the grid size, which can be regarded as the average distance between two neighboring nodes for irregular grid arrangement. For regular grid pattern, it is the adjacent nodal spacing.

Firstly, the convergence of the present method is carried out. Since the governing equations have the second order partial derivatives with respect to x and y , the basis function should be at least of the same order of completeness, i.e., the monomial basis should be selected from a quadratic order polynomial or higher. For simplicity, the completeness order of the basis functions \tilde{N} is taken to be 2 in our computation. The grid point pattern used in this study is distributed regularly as shown in Fig. 2. The convergence characteristics of center deflection parameter $W^* = 10hW/(\alpha_x \tilde{T}a^2)$ for such a plate at time $t = 1s$, $m = n = 1$, are presented in Table 1, respectively, as the distribution is increased from 9×9 to 15×15 discrete nodes at various scaling factors d_{\max} . It is seen from this

Table 1 Convergence characteristics of center deflections W^* at $t = 1s$ for a three layered cross ply laminated square plate having four simply supported boundary conditions ($E_1 = 25E_2$, $G_{12} = G_{13} = 0.5E_2$, $G_{23} = 0.2E_2$, $\nu = 0.25$)

d_{max}	N	$h/a = 0.01$			$h/a = 0.2$		
		$a/b = 0.5$	$a/b = 1$	$a/b = 2$	$a/b = 0.5$	$a/b = 1$	$a/b = 2$
4	9×9	0.8134e-5	0.9615e-5	0.1559e-4	0.120878	0.388801	0.507802
	11×11	0.8358e-5	0.9742e-5	0.1565e-4	0.121615	0.393688	0.512106
	13×13	0.8439e-5	0.9937e-5	0.1579e-4	0.123478	0.396840	0.514391
	15×15	0.8540e-5	0.9945e-5	0.1586e-4	0.125756	0.396837	0.515227
5	9×9	0.8402e-5	0.9733e-5	0.1453e-4	0.123402	0.389429	0.508269
	11×11	0.8483e-5	0.9867e-5	0.1565e-4	0.126697	0.394415	0.513367
	13×13	0.8559e-5	0.9955e-5	0.1589e-4	0.127423	0.397638	0.514692
	15×15	0.8563e-5	0.9986e-5	0.1618e-4	0.128682	0.398825	0.518887
6	9×9	0.8412e-5	0.9941e-5	0.1455e-4	0.126568	0.392147	0.509089
	11×11	0.8506e-5	0.9896e-5	0.1582e-4	0.128943	0.395289	0.512728
	13×13	0.8528e-5	0.9968e-5	0.1604e-4	0.128627	0.396467	0.515555
	15×15	0.8566e-5	0.9984e-5	0.1618e-4	0.128874	0.398895	0.518869

Table that with increasing the number of grid points, the center deflection is converged to certain values monotonically for different scaling factor d_{max} . However, the convergence rate for a larger scaling factor is faster than that for a lower one, whatever the thickness of the plate. Generally speaking, in order to avoid the matrix singularity and ensure smoothness of the MLS shape functions and its partial derivatives, more discrete points in the influence domain, i.e., larger support size than the lower case, should be used. It is also found that the convergence rate is better for a thick plate than for a thin plate, when the same grid point and the same scaling factor are used. For a thin plate ($h/a = 0.01$) with a scaling factor $d_{max} = 4$, the relative discrepancy of the center deflection between grid 9×9 and 15×15 is 4.7%, 3.3% and 1.7%, respectively, for the aspect ratio $a/b = 0.5$, $a/b = 1$ and $a/b = 2$; while for a thick plate with the same scaling factor, the relative discrepancy of the center deflection is 3.8%, 2.0% and 1.4%, respectively, for the same aspect ratio. In the following studies, 11×11 grid points and the scaling factor $d_{max} = 5$ are used for saving the computation time.

Table 2 Comparisons of center deflections W^* at $t = 1$ sec for a three layered cross ply laminated square plate having four simply supported boundary conditions at lowest heat flux frequency ζ under various vibration mode ($E_1 = 25E_2$, $G_{12} = G_{13} = 0.5E_2$, $G_{23} = 0.2E_2$, $\nu = 0.25$)

h/a		0.01	0.02	0.05	0.1	0.2
ω_{11}	Present solutions	0.986775e-5	0.163125e-3	0.148074e-2	0.200838e-1	0.394415
	Hong <i>et al.</i> (2003)	0.102052e-4	0.163578e-3	0.148182e-2	0.200950e-1	0.399904
ω_{22}	Present solutions	0.101485e-4	-0.845964e-5	0.174381e-2	0.637205e-1	0.796148
	Hong <i>et al.</i> (2003)	0.103904e-4	-0.867549e-5	0.177562e-2	0.639221e-1	0.798220
ω_{33}	Present solutions	0.105479e-4	0.431389e-4	0.331446e-2	0.130706	1.12038
	Hong <i>et al.</i> (2003)	0.106990e-4	0.432117e-4	0.333286e-2	0.130818	1.12156

Next, comparison studies are also made for the center deflections W^* of a simply supported square plate. The material properties and the plate size as well as the stacking sequence of the plate are all the same with those in convergency studies. The results are tabulated in Table 2. It is found that the present results are in close agreement with those given by Hong *et al.* using the GDQ method.

Figs. 3-5 show the variation of the non-dimensional center deflection amplitude $W^* = 10hW/(\alpha_x \tilde{T} a^2)$ with respect to side-to-thickness ratio a/h , under the lowest three vibration frequencies $\omega_{11}, \omega_{22}, \omega_{33}$, lowest frequency of applied heat flux ζ , at time $t = 1, 2, \dots, 5s$, for a square cross ply laminated plate $[0^\circ/90^\circ/0^\circ]$ subjected to thermal vibration of time sinusoidal temperature distribution. It is found that the transverse deflection amplitude decreases rapidly by increasing the side-to-thickness ratio a/h , especially in the range $a/h < 20$. For the cases $a/h > 20$, the transverse deflection amplitude changes very slowly. It is also found that with increasing the vibration frequency from ω_{11} to ω_{33} , the deflection parameters W^* have a slight increase; however, the differences of the deflection parameters between three vibration frequencies $\omega_{11}, \omega_{22}, \omega_{33}$ are very small.

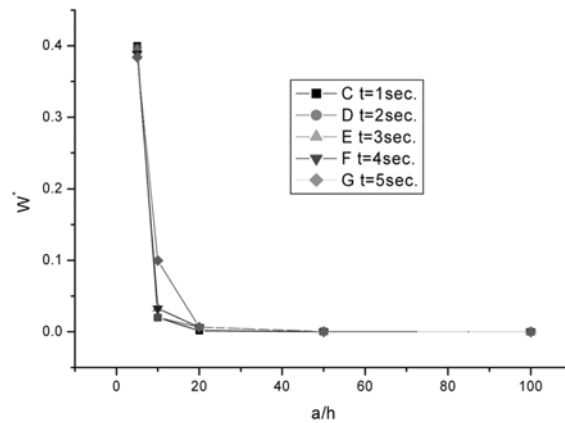


Fig. 3 Center deflection amplitude W^* w.r.t. a/h under ω_{11} , lowest ζ at various time

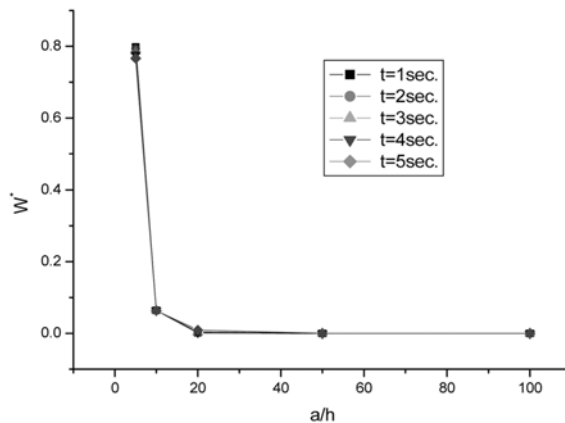


Fig. 4 Center deflection amplitude W^* w.r.t. a/h under ω_{22} , lowest ζ at various time

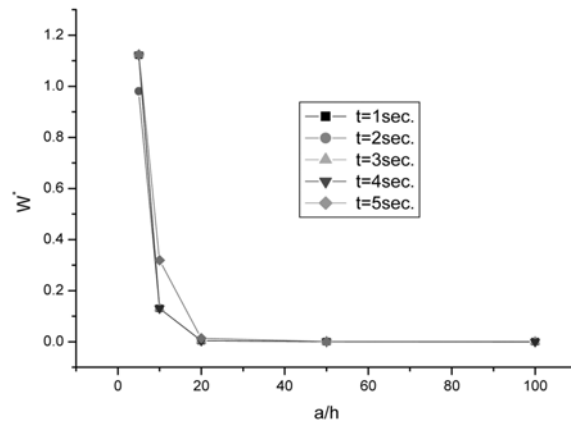


Fig. 5 Center deflection amplitude W^* w.r.t. a/h under ω_{33} , lowest ζ at various time

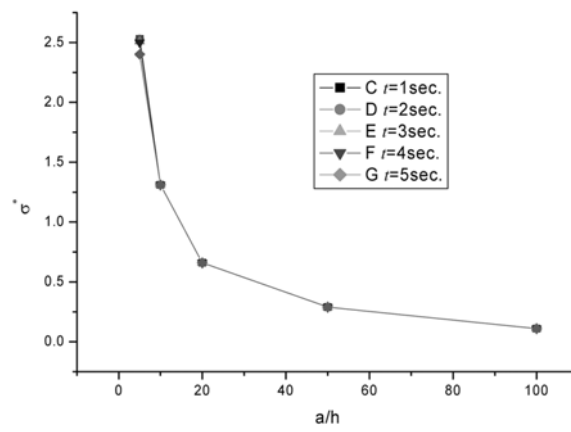


Fig. 6 Stress amplitude σ_y^* w.r.t. a/h under ω_{11} , lowest ζ at various time

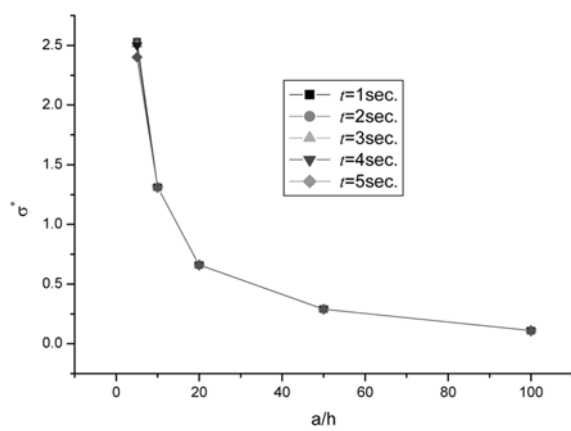


Fig. 7 Stress amplitude σ_y^* w.r.t. a/h under ω_{22} , lowest ζ at various time

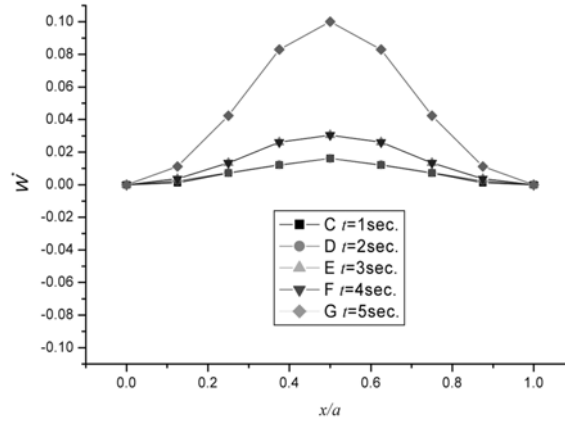


Fig. 8 Deflection amplitude W^* distribution along x -axis at $y = 0.5b$ under ω_{11} , lowest ζ at various time

Figs. 6 and 7 plot the variation curves of the non-dimensional stress $\sigma_y^* = \sigma_y h / (\alpha_x a E_2 \tilde{T})$ at center position of the first interface with the side to thickness ratio a/h under the lowest natural frequencies ω_{11} and ω_{22} , respectively, of the plate, lowest frequency of applied heat flux ζ , at time $t = 1, 2, \dots, 5s$, for a square laminated plate with stacking sequence $[0^\circ/90^\circ/0^\circ]$ subjected to thermal vibration of time sinusoidal temperature distribution. It is seen that the stress σ_y^* decreases as increasing the side to thickness ratio. Also, the difference of the stress parameter between ω_{11} and ω_{22} is very small. It is evident that the values of stresses σ_y^* in ω_{22} case are almost the same as those in the case ω_{11} .

Fig. 8 illustrates the variation trend of the non-dimensional transverse deflection time response curve with the side x/a under the lowest natural frequency ω_{11} of the plate, lowest frequency of applied heat flux ζ , at time $t = 1, 2, \dots, 5s$, for a square cross ply laminated plate $[0^\circ/90^\circ/0^\circ]$ subjected to thermal vibration of time sinusoidal temperature distribution. The side to thickness ratio is taken as $a/h = 10$. It is obvious that the center deflection amplitude increases when x/a changes from 0.0 to 0.5, then decreases when x/a changes from 0.5 to 1.0. The transverse deflection is almost on the same curve at time $t = 1, 2, 3s$. One can easily find that the largest center deflection is found at the center of the plate.

8. Conclusions

In this paper, the moving least-squares differential quadrature method has been applied successfully to solve the dynamic response for deflections and stresses of a cross ply laminated moderately thick plate with simply supported boundary conditions, subjected to thermal load which is a sinusoidal time function. This is the first endeavor to exploit the MLSAQ method for thermal vibration analysis of thick laminated plates. Several examples have been selected to demonstrate the convergency and applicability of the present MLSAQ procedures. It has been shown that the MLSAQ method yields rapidly convergent and accurate solutions for calculating the deflections and stresses in a multi-layered plate of cross ply laminate with a rectangular domain including shear deformation with a few grid points. It is also concluded that larger support size than lower one can often generate results with better accuracy when same discretization and same basis functions are

used. Some new results show that the deflection and stress parameters decrease with increasing the side to thickness ratio a/h , especially in the range $a/h < 20$. There are very small differences for deflection parameters and stress parameters between three natural frequencies ω_{11} , ω_{22} , ω_{33} .

References

- Baharlou, B. and Leissa, A.W. (1987), "Vibration and buckling of generally laminated composite plates with arbitrary edge conditions", *Int. J. Mech. Sci.*, **28**, 545-555.
- Bellman, R.E. and Casti, J. (1971), "Differential quadrature and long term integration", *J. of Mathematical Analysis and Applications*, **34**, 235-238.
- Bellman, R.E. and Casti, J. (1972), "Differential quadrature: A technique for the rapid solution of nonlinear partial differential equations", *J. of Computational Physics*, **10**, 40-52.
- Belytschko, T., Lu, Y.Y. and Gu, L. (1994), "Element-free Galerkin methods". *Int. J. Numer. Meth. Eng.*, **37**, 229-256.
- Bert, C.W. and Malik, M. (1996), "Differential quadrature method in computational mechanics: A review", *Applied Mechanics Review*, **48**, 1-28.
- Civan, F. (1994), "Solving multivariable mathematical models by the quadrature and cubature methods", *Numerical Method for Partial Differential Equations*, **10**, 545-567.
- Hetnaski, R.B. (1986), *Therma Stresses*. Amsterdam, Elsevier.
- Hong, C.C. and Jane, K.C. (2003), "Shear deformation in thermal vibration analysis of laminated plates by the GDQ method", *Int. J. Mech. Sci.*, **45**, 21-26.
- Huang, X.L., Shen, H.S. and Zheng, J.J. (2004), "Nonlinear vibration and dynamic response of shear deformable laminated plates in hygrothermal environments", *Composite Science and Technology*, **64**, 1419-1435.
- Jonnalagadda, K.D., Blandford, G.E. and Tauchert, T.R. (1994), "Piezothermoelastic composite plate analysis using first-order shear deformation theory", *Comput. Struct.*, **51**, 79-89.
- Kabir, H.R.H. and Chaudhuri, R.A. (1994), "Free vibration of clamped, moderately thick, arbitrarily laminated plates using a generalized Navier's approach", *J. Sound Vib.*, **171**, 397-410.
- Kabir, H.R.H. (1999), "On the frequency response of moderately thick simply supported rectangular plates with arbitrarily lamination", *Int. J. Solids Struct.*, **36**, 2285-2301.
- Liew, K.M. (1996), "Solving the vibration of thick symmetric laminates by Reissner/Mindlin plate theory and the p -Ritz method", *J. Sound Vib.*, **198**, 343-360.
- Liew, K.M., Han, J.B. and Xiao, Z.M. (1996), "Differential quadrature method for Mindlin plates on Winkler foundations", *Int. J. Mech. Sci.*, **38**, 405-421.
- Liew, K.M., Huang, Y.Q. and Reddy, J.N. (2002), "A hybrid moving least squares and differential quadrature meshfree method", *Int. J. Comput. Eng. Sci.*, **3**, 1-12.
- Liew, K.M., Huang, Y.Q. and Reddy, J.N. (2003), "Moving least squares differential quadrature method and its application to the analysis of shear deformable plates", *Int. J. Numer. Meth. Eng.*, **56**, 2331-2351.
- Malik, M. and Bert, C.W. (1998), "Three dimensional elasticity solutions for free vibrations of rectangular plates by the differential quadrature method", *Int. J. Solids Struct.*, **35**, 299-381.
- Wang, X., Wang, Y.X. and Yang, H.K. (2005), "Dynamic inter-laminar stresses in laminated plates with simply and fixed supports, subjected to free vibrations and thermal load", *Comp. Struct.*, **68**, 139-145.
- Wang, X. and Zhang, Y.C. (2005), "Transient response of inter-laminar stresses in laminated plates with complex boundary, under thermal environment", *J. of Reinforced Plastics and Composites*, **24**, 93-109.
- Whiney, J.M. (1987), *Structural Analysis of Laminated Anisotropic Plates*. Lancaster, PA, USA: Technomic Publishing Company, Inc.